

The Synthesis and Phosphate Adsorptive Properties of Mg(II)–Mn(III) Layered Double Hydroxides and Their Heat-Treated Materials

Satoko Tezuka,[1,2,†] **Ramesh Chitrakar,**[1,†] **Kohji Sakane,**[1,†] **Akinari Sonoda,**[1,†] **Kenta Ooi,**[*,1,†] **and Tahei Tomida**[2]

[1]Institute for Marine Resources and Environment, National Institute of Advanced Industrial Science and Technology (AIST), 2217-14 Hayashi-cho, Takamatsu 761-0395

[2]The University of Tokushima, 2-1 Minamijosanjima, Tokushima 770-0814

Received January 13, 2004; E-mail: k-ooi@aist.go.jp

Hydrotalcite-like layered double hydroxides (LDHs) of Mg(II) and Mn(III) were prepared by a co-precipitation/air oxidation method using $MgCl_2$ and $MnCl_2$ as starting materials. Syntheses were studied at different precipitation temperatures and variable starting Mg/Mn ratios. MgMn-LDH were obtained at a preparation temperature below 333 K. Samples prepared at a Mg/Mn ratio of 3 showed a crystalline LDH phase having a basal spacing of 7.85 Å. The LDH prepared at lower Mg/Mn ratios had slightly less crystalline phase, with lower basal spacing. Calcination of MgMn-LDH at 573 K for 4 h in air resulted in a transformation from a layered to an amorphous phase, accompanied by a loss of interlayer water and a partial loss of carbonate ions. Chemical analysis and IR studies showed that oxidation from Mn(III) to Mn(IV) progressed during the calcinations, and that HCO_3^- was formed in the calcined solid. Equilibrium distribution coefficients (K_d) of different kinds of anions were measured for the uncalcined and calcined samples. The selectivity sequences were $Cl^- < NO_3^- < SO_4^{2-} < HPO_4^{2-}$ and Cl^-, NO_3^-, $SO_4^{2-} \ll HPO_4^{2-}$ for the uncalcined and calcined ones, respectively. The latter had specific selectivity for phosphate ions. The calcined sample showed a maximum phosphate uptake of 1.1 mmol-P/g at a pH around of 8. The pH titration study of the supernatant solution suggested that the phosphate adsorption progresses mainly through the HCO_3^-/HPO_4^{2-} ion exchange reaction.

Hydrotalcite (aluminum magnesium carbonate hydroxide hydrate) is a common mineral found in nature. It consists of positively charged layers, which are partially substituted by Al^{3+} cations in octahedral brucite $Mg(OH)_2$ layers separated by carbonate anions and water molecules in the interlayer space in order to maintain the electrical neutrality of the compound. The first exact formula for hydrotalcite was proposed to be $Mg_6Al_2(OH)_{16}CO_3 \cdot 4H_2O$.[1] In recent years, layered double hydroxides (LDHs) known as anionic clays or hydrotalcite-like compounds have attracted a great deal of attentions due to their possible use as adsorbents, separation media, catalysts, etc.[1–13] The general formula describing the chemical composition of LDHs is $[M(II)_{1-x}M(III)_x(OH)_2]^{x+}[(A^{z-})_{x/z} \cdot nH_2O]$, where M(II) = Mg, Mn, Co, Ni, Cu, Zn, and M(III) = Al, V, Cr, Mn, Fe, Co, and Ga, and $A^{z-} = OH^-$, Cl^-, NO_3^-, and CO_3^{2-}. In general, cations having an ionic radius similar to that of Mg^{2+} can be substituted in the Mg sites of the brucite layers, thus leading to the formation of LDHs. There have been claims that LDHs can be prepared with x values of 0.1–0.5 in the above general formula, but that the value may be only for a narrow range ($0.20 < x < 0.33$).[7]

Phosphate ion adsorbents are very important in the medical area (for the prevention of hyperphosphatamia)[14] and in lake and seawater environmentals.[5,15] Most phosphorus pollution in lakes and seawater is from wastewater generated by industries, household chemicals, and fertilizers. The red tide caused by eutrophication in lakes and ocean is an important problem. When the concentration of phosphate in lakes or ocean is over 0.03 mg/dm^3, a red tide occurs. Adsorption using inorganic ion exchange materials is a promising technique, that is useful in phosphate removal. In the past, a wide variety of LDHs have been studied in terms of the removal of phosphate ions, MgAl-LDHs being the most studied compound. However, most LDHs do not show a specific selectivity for phosphate ions alone, other divalent anions such as sulfate and carbonates are also preferred.[3,16] Therefore, they cannot effectively remove hazardous phosphate from seawater. We are interested in MgMn-LDH as a selective adsorbent for phosphate ions for the following reasons: 1) MgMn-LDHs are stable enough in an alkaline solution, which is advantageous during the phosphate desorption, 2) Mn compounds are cheap compared to Zn or Cr compounds. The common phosphate adsorbent MgAl-LDH suffers from the dissolution of Al at high pH during phosphate desorption. Sample MgFe-LDH does not have a high selectivity for phosphate ion alone in multi anion solutions.

Desautelsite, a mineral of Mg(II) and Mn(III) carbonate hydroxide was, first reported by Dunn et al.[17] Hansen and Taylor[18] described the preparation of MgMn-LDH by airing a suspension of $MnCO_3$ in $Mg(NO_3)_2$ solution at pH 9 and 308 K. However, if lower synthesis temperatures were used (298 K), unreacted $MnCO_3$ coexisted with hausmanite ($Mn^{III}O_4$). To the best of our knowledge, there have been no

† Current research unit: Research Institute for Environmental Management Technology

Published on the web November 11, 2004; DOI 10.1246/bcsj.77.2101

detailed studies on the preparation of MgMn-LDH with Mn(III) from a $MgCl_2$–$MnCl_2$ mixed solution, not have there have been any studies on the oxo-anion adsorptive properties of MgMn-LDH. In this paper, we found that MgMn-LDH and its calcined materials displayed interesting adsorption properties towards phosphate ions.

Experimental

Synthesis. Hydrated metal chlorides of high purity (99%) were supplied by Wako Chemical Co., Japan. Other reagents were all of analytical grade. A mixed solution (100 cm^3) containing 0.03 M Mg(II) and 0.01 M Mn(II) (1 M = 1 mol dm^{-3}) was slowly added drop-wise to a solution (100 cm^3) containing 0.2 M NaOH and 0.1 M Na_2CO_3, which was stirred magnetically. The resultant suspensions were stirred for over 2 h, and the precipitates were separated by centrifugation and washed repeatedly with deionized water until neutral, then air-dried at room temperature. Samples MgMn-1, MgMn-2, MgMn-3, MgMn-4, and MgMn-5 were synthesized at 275, 293, 313, 333, and 353 K, respectively, at a Mg/Mn ratio of 3. Samples MgMn-6 and MgMn-7 were synthesized with Mg/Mn ratios of 2 and 1, respectively, at 293 K. Calcined samples were prepared by heating MgMn-2, MgMn-6, and MgMn-7 at 573 K for 4 h in air. They are designated as MgMn-2-573, MgMn-6-573, and MgMn-7-573, respectively.

Characterization. Powder X-ray diffraction analysis was carried out using a Rigaku X-ray Diffractometer (RINT 1200) equipped with Ni-filtered Cu Kα radiation (λ = 1.5404 Å) and graphite monochromator. The data were collected at room temperature in the range of 2θ between 5° and 70° with a scan rate of 1° (2θ)/min. Lattice parameters were refined by the least squares method. The errors were ±0.01 Å for both lattice parameters a and c. TG-DTA experiments were conducted on a MAC Science Thermal Analyzer (200 TG-DTA) at a heating rate of 283 K/min in air. Infrared spectra were recorded by the KBr pellet method using a Perkin Elmer FT-IR Spectrometer (Spectrum 2000). SEM observations were carried on a Hitachi Natural Scanning Electron Microscope (S-2460 N).

Chemical Analysis. Manganese and magnesium content was determined using a Shimadzu Atomic Absorption Spectrometer (AA-670) after dissolving a powder sample (0.05 g) in a 0.5 M HCl solution followed by the addition of a few drops of H_2O_2. The mean oxidation state of manganese (Z_{Mn}) was evaluated after determining the available oxygen by the standard oxalic acid method.[19] A 3.5 M sulfuric acid solution (10 cm^3) and a standard 0.3 M sodium oxalate solution (10 cm^3) were poured into a powder sample (0.10 g). After dissolving the sample at 363 K in a water bath, the excess sodium oxalate was back titrated with a standard 0.1 M potassium permanganate solution. The water content was calculated from the weight loss by heating at 473 K. CO_2 and Cl content was determined by gas chromatography with a Horiba EMIA-U511 analyzer.

Adsorption Experiments. Equilibrium distribution coefficients (K_d) of the oxo-anion were determined by a batch method. A powder sample (0.10 g) was immersed in a mixed solution (10 cm^3) of NaCl, $NaNO_3$, Na_2SO_4, and NaH_2PO_4 (2×10^{-3} M each). After attainment of equilibrium (3 d), the resultant solution was filtered, and concentrations of Cl^-, NO_3^-, SO_4^{2-}, and HPO_4^{2-} remaining in the solution were determined by ion chromatography with a Shimadzu type LC-10Ai apparatus. The amounts of anions adsorbed were calculated from the concentrations relative to the initial concentrations. The K_d values were calculated using the following equation:

$$K_d\ (cm^3/g) = \frac{[\text{Anion adsorbed (mg/g of solid)}]}{[\text{Final anion concentration (mg/cm}^3\text{ of solution)}]}. \quad (1)$$

The pH dependence of phosphate adsorption on MgMn-2-573 was also studied by a batch method. A calcined sample (0.10 g) was immersed in a 4×10^{-3} M NaH_2PO_4 solution (50 cm^3), and the pH of the solution was adjusted using a 0.1 M HCl or a 0.1 M NaOH solution. After attainment of equilibrium (3 d), the solid was separated by filtration and air-dried at room temperature. The amount of phosphate adsorbed was determined using a Seiko ICP Atomic Emission Plasma Spectrometer (SPS 7800) after dissolving a known weight of the solid in a 0.5 M HCl solution containing 2% H_2O_2. The pH titration of the supernatant solution after phosphate adsorption was carried out for MgMn-2-573 by the conventional method. After the solid sample (0.10 g) was mixed with a 0.1 M Na_2HPO_4 solution (20 cm^3) for 2 d, the solid was separated by filtration, and the supernatant solution was titrated with a 0.1 M HCl solution.

Results and Discussion

Chemical Analysis. Chemical analysis results are given in Table 1. The Mg/Mn mole ratios are about 3 for samples from MgMn-1 to MgMn-5, 1.97 for MgMn-6, and 0.97 for MgMn-7. These values are acceptably close to those in the starting solutions. The mean oxidation numbers (Z_{Mn}) of manganese were in the range between 3.02 and 3.16, indicating that oxidation from Mn(II) to Mn(III) progressed completely during the preparation. The chemical composition was calculated for MgMn-2, MgMn-6, and MgMn-7 prepared at 293 K using the Mg, Mn, CO_2, Cl, and H_2O contents, as is shown in Table 1. The Cl contents are markedly smaller than the CO_2 contents, indicating that the interlayer anions are mainly carbo-

Table 1. Chemical Analysis of MgMn-LDHs and Their Compositions

Sample	Preparation conditions		Mole ratio of solid				Z_{Mn}	Chemical composition	AEC
	Temp./K	Mg/Mn	Mg/Mn	H_2O/Mn	CO_2/Mn	Cl/Mn			mequiv./g
MgMn-1	275	3.00	3.09	3.2	—	—	3.04	—	—
MgMn-2	293	3.00	3.03	3.2	0.60	0.005	3.02	$[Mg_{0.75}Mn_{0.25}(OH)_2][(CO_3)_{0.15}Cl_{0.02}\cdot 0.80H_2O]$	3.4
MgMn-3	313	3.00	3.10	3.2	—	—	3.03	—	—
MgMn-4	333	3.00	3.03	2.6	—	—	3.08	—	—
MgMn-5	353	3.00	3.06	—	—	—	3.16	—	—
MgMn-6	293	2.00	1.97	2.6	0.48	0.012	3.02	$[Mg_{0.67}Mn_{0.33}(OH)_2][(CO_3)_{0.16}Cl_{0.04}\cdot 0.85H_2O]$	3.5
MgMn-7	293	1.00	0.97	1.6	0.35	0.008	3.04	$[Mg_{0.49}Mn_{0.51}(OH)_2][(CO_3)_{0.18}Cl_{0.04}\cdot 0.81H_2O]$	3.7

Z_{Mn}: Mean oxidation state of manganese. AEC: Anion exchange capacity calculated from a sum of carbonate and chloride contents.

nate ions. Anion exchange capacities (AEC) were calculated from the CO_2 and Cl contents assuming a pure LDH structure and interlayer anions of CO_3^{2-} and Cl^-.

X-ray Diffraction Analysis. All samples except for MgMn-5 had XRD patterns typical of a LDH structure, with sharp and symmetric reflections corresponding to basal planes (003), (006), and (009), and broad and asymmetric reflections for non-basal planes (012), (015), and (018) (Fig. 1). The Miller indexing in Fig. 1 is referred to as a hexagonal lattice with a rhombohedral lattice with *R*3*m* symmetry. The crystallinity of LDH depends on the preparation temperature. The peak intensity of each reflection was almost the same for samples (MgMn-1, MgMn-2, and MgMn-3) prepared below 313 K, while it weakened for MgMn-4 prepared at 333 K. The brucite $Mg(OH)_2$ phase was predominant for MgMn-5 prepared at 353 K. This preparation-temperature dependence is different from those observed in conventional LDHs. Usually, the crystallinity of LDH increases with an increase in the synthesis temperature.[20] In the present case, the oxidation of Mn(II) to Mn(III) is needed in addition to the simple hydrolysis of Mg(II) and Mn(II) ions. Since the oxidation progresses using dissolved oxygen, the oxidation rate depends strongly on the oxygen concentration of the reaction solution. It may be high enough at low temperatures to oxidize Mn(II) effectively, while it may be insufficient at temperatures above 333 K due to a decrease in oxygen concentration. At this point, a competitive reaction with $Mg(OH)_2$ crystallization may progress during aging. The XRD pattern of MgMn-7 shows small peaks at 19.2°, 32.6°, and 36.0° (2θ), which were assigned to the MnO(OH) phase (JCPDS No. 18-0804).

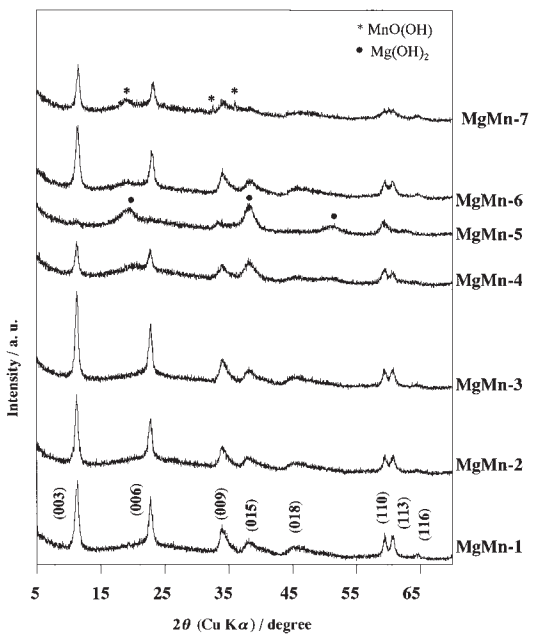

Fig. 1. Powder X-ray diffraction patterns of MgMn-LDHs.

The structural parameters of MgMn-2, MgMn-6, and MgMn-7 are given in Table 2. The lattice parameters of MgMn-1 and MgMn-3 were almost the same as those of MgMn-2. The parameter *a* is the average distance between two cations in the brucite layer, and *c* is 3 times the distance from a layer to the next layer. There was no appreciable difference in the *a* value with the isomorphous substitution of Mg(II) by Mn(III) in the brucite layer because of the equal ionic radii of these two cations. The *c* value increased slightly with the isomorphous substitution of Mg(II) by Mn(III) (with increasing Mg/Mn ratio). Since the *c* value depends on the interlayer distance, it was influenced by the charge density of the layer, the nature of the interlayer anion, and the amount of interlayer water. The charge density, calculated from the chemical composition data, increased with an increase in the Mn content (Table 2). Therefore, the decrease in the *c* value with the isomorphous substitution (with a decrease in the Mg/Mn ratio) can be explained by the increase in Coulombic attractive force between the positively charged brucite layers and the negative carbonate anions.

Characterization of Calcined Samples. XRD patterns of MgMn-2 calcined at different temperatures for 4 h in air are shown in Fig. 2. Calcination at 473 K resulted in a slight shift of the (003) reflection peak to a lower *d* value, from 7.8 to 6.3 Å. In addition, the (006) reflection disappeared and the intensity of the (009) reflection decreased considerably. The broadness of the (003) reflection and the disappearance of the (006) reflection suggests a disordering of the stacked layers of LDH. Calcination at 573 or 673 K resulted in the collapse of the layered structure to form a nearly amorphous phase, similar to the case of other LDH samples.[2] The peaks corresponding to the oxide phase (Mg_2Mn_4, MgO, or Mn_2O_3) are observed clearly for the sample calcined at 873 K. The diffraction peaks become sharpen and stronger by further calcination at 1073 K. The splitting of the peak around 60° to 57° and 63° suggests that MgMn-2-1073 consists mainly of a mixture of Mg_2MnO_4 (JCPDS No. 19-0773) and MgO (JCPDS No. 4-0829).

Chemical analysis of MgMn-2-573 gave the mole ratios of $Mg/Mn = 3.02$, $CO_2/Mn = 0.48$, and $H_2O/Mn = 0.57$. Nearly 25% of the CO_2 and most of the H_2O molecules dissipated from the solid by the heating at 573 K. The Z_{Mn} value

Table 2. Structural Parameters of MgMn-LDHs Prepared at 293 K

Parameter	MgMn-2	MgMn-6	MgMn-7
Mn(III) substitution in brucite layer[a)]	0.25	0.33	0.51
Basal spacing/Å	7.85	7.78	7.69
Unit cell, a/Å	3.11	3.11	3.10
c/Å	23.8	23.7	23.6
Layer unit area/Å^{2} [b)]	8.37	8.37	8.32
Layer charge density/e$^+$ Å^2	0.030	0.039	0.061

a) Determined by chemical analyses of Mg and Mn contents. b) Area of $Mg_{1-x}Mn_x(OH)_2$ octahedral unit $= [3(a^2/2)]^{1/2}$.

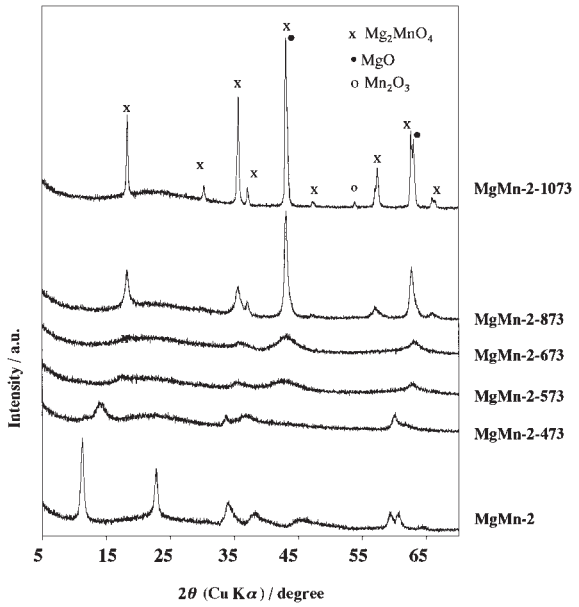

Fig. 2. Powder X-ray diffraction patterns of MgMn-2 calcined at different temperatures.

was determined to be 4.0. This shows that the oxidation of Mn(III) to Mn(IV) progresses during the heat treatment. The surface properties of MgMn-2-573 were studied by nitrogen absorption–desorption at 77 K. The isotherm belonged to type IV in the IUPAC classification with a small hysteresis loop, indicating the presence of mesopores. The BET surface area was 68 m^2/g.

It is noticeable that sample MgMn-2-573 did not return to a layered structure after immersion in water, in contrast to the case of MgAl and MgFe-LDH samples. They transform to an amorphous structure by calcinations at 673 K, but return to the layered structure after subsequent immersion in water or an aqueous solution.[20] In the present case, the oxidation of skeletal Mn(III) to Mn(IV) may be caused by a destruction of the local layered structure.

Thermal Analysis. The TG-DTA curves for MgMn-2, MgMn-6, and MgMn-7 and the non-LDH sample MgMn-5 are shown in Fig. 3. The thermal behaviors of other samples (MgMn-1, MgMn-3, and MgMn-4) were almost the same as that of MgMn-2. The DTA curves of MgMn-2 showed two endothermic peaks around 426 and 583 K, associated with two stages of weight loss. According to the DTA-TG results of LDHs in the literature,[20] the first endothermic peak around 426 K can be assigned to the dissipation of interlayer water molecules and the second one at 583 K to the dissipation of the hydroxide groups of the metal hydroxide layer and interlayer carbonate anions.

Samples MgMn-6 and MgMn-7 also showed two endothermic peaks around 400 and 600 K. These two DTA peaks were shifted to slightly lower temperatures with a decrease in the Mg/Mn ratio. The XRD pattern of MgMn-7-573 had a spinel-type structure with the strongest peak around 19°. Since they have larger Mn content than MgMn-2-573, the thermal oxidation of skeletal Mn may result in the acceleration of the structural transformation.

FT-IR Analysis. MgMn-LDHs showed the IR spectra

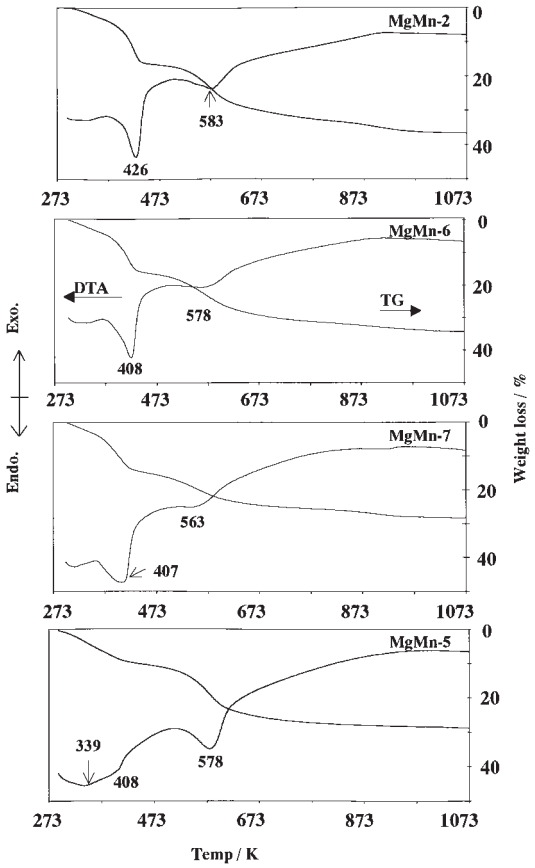

Fig. 3. TG-DTA curves of MgMn-LDHs with different Mg/Mn ratios.

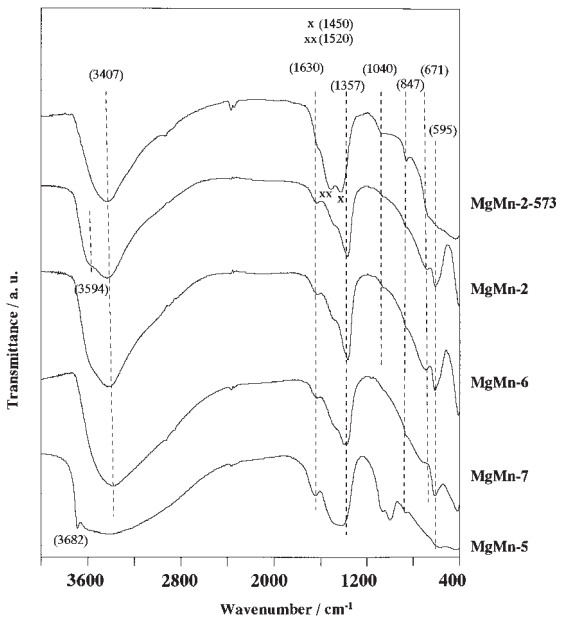

Fig. 4. IR spectra of MgMn-LDHs with different Mg/Mn ratios.

typical of LDH compounds, except for MgMn-5 (Fig. 4). The main bands were in the same positions independent of the Mg/Mn mole ratio. In addition to the common broad band around 3400 cm^{-1}, a shoulder was observed at around 3600 cm^{-1} for sample MgMn-2. These two bands can be assigned

to OH stretching vibrations of the hydroxy groups in the layers and interlayer water molecules. The bending mode of the interlayer water molecules is responsible for a small intense band recorded at 1630 cm^{-1}. Sharp and strong bands at ca. 1357 cm^{-1} in the spectra of MgMn-2 and MgMn-6 were due to the ν_3 mode of CO_3^{2-} anions in a symmetric environment in the interlayer space.[21] This band split into a doublet for sample MgMn-7 with a maxima at 1353 cm^{-1} and 1373 cm^{-1}, which can be attributed to a lowering of the symmetry of carbonate anion.[20] The bands (671 and 595 cm^{-1}) recorded below 800 cm^{-1} were due to the lattice vibrations of the M–O crystal (M = Mg, Mn). The non-LDH sample MgMn-5 had a small, sharp peak at 3680 cm^{-1}, which can be assigned to the stretching vibration of the hydroxy group in the brucite $Mg(OH)_2$ structure.

The IR spectrum of MgMn-2-573 has bands at 1450 and 1520 cm^{-1}. The band at 1450 cm^{-1} can be assigned to the vibration of bicarbonate (HCO_3^-) ions.[22] This suggests that the major chemical species of carbonate in MgMn-2-573 is HCO_3^-. On the basis of the chemical analysis and IR results, the composition of MgMn-2-573 can be written as $Mg_{0.75}Mn_{0.25}O_{1.21}(HCO_3)_{0.12}(H_2O)_{0.10}$. Since HCO_3^- ion is thermally less stable than CO_3^{2-}, the transformation from CO_3^{2-} to HCO_3^- may hardly occur at 573 K during calcination. The HCO_3^- ions may be formed after cooling by the reaction of H_2O molecules with the residual CO_2 on the metal oxide surface. It is well known that the adsorption of H_2O on the surface of metal oxides results in the formation of surface hydroxy groups with an amphoteric nature.[23,24] The basic hydroxy group can react with residual CO_2 to form HCO_3^- ions.

Scanning Electron Microscopy. The SEM images of MgMn-2, MgMn-6, and MnMn-7 and the calcined sample MgMn-2-573 are presented in Fig. 5. All of the samples showed the morphology of plate-like particles stacked on the top of each other in parallel arrangement. Sample MgMn-2-573 still preserved the initial morphology even after calcinations, although the crystal structure changed from layered to amorphous.

Equilibrium Distribution Coefficients (K_d). The K_d values of oxo-anions from a mixed anion solution containing Cl^-, NO_3^-, SO_4^{2-}, and HPO_4^{2-} are presented in Table 3. The selectivity sequence was $Cl^- < NO_3^- < SO_4^{2-} < HPO_4^{2-}$ for the uncalcined samples. Normally, selectivity in ion exchange increases with an increase in the valence of the adsorbing anion due to the increase in electrostatic interactions between

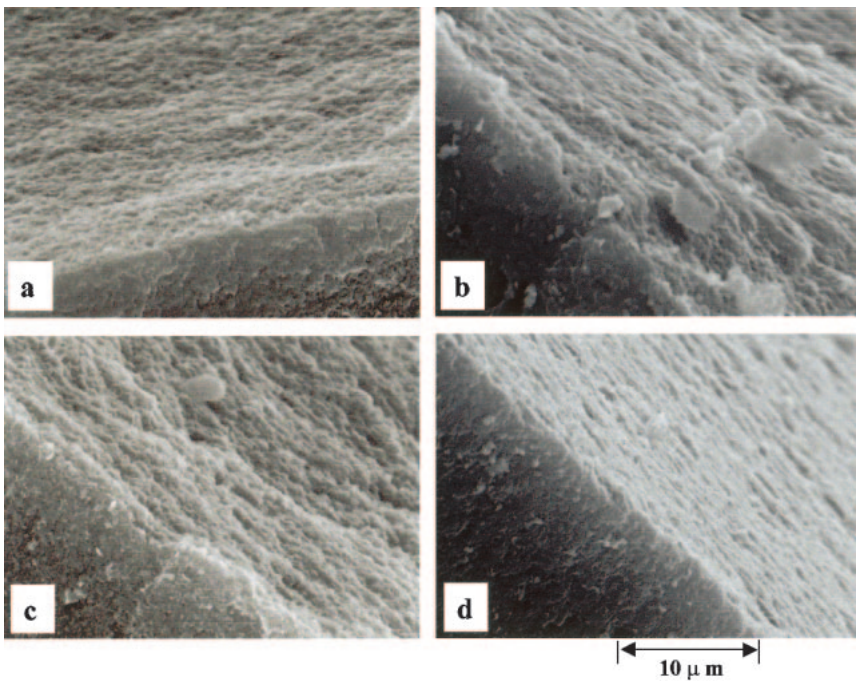

Fig. 5. SEM images of MgMn-LDHs. (a) MgMn-2, (b) MgMn-2-573, (c) MgMn-6, (d) MgMn-7.

Table 3. Distribution Coefficients of Anions

Sample	Distribution coefficient (K_d)					pH
	CO_3^{2-}	Cl^-	NO_3^-	SO_4^{2-}	HPO_4^{2-}	
MgMn-2	<1	2	6	37	140	9.8
MgMn-6	<1	<1	5	25	500	9.9
MgMn-7	<1	<1	6	18	4500	9.9
MgMn-2-573	<1	<1	6	9	$>10^4$	10.8
MgMn-6-573	<1	<1	<1	<1	$>10^4$	10.8
MgMn-7-573	<1	<1	4	<1	190	10.5

ion-exchange sites and anions.[25] The present uncalcined samples also follow this tendency in that they prefer divalent anions to monovalent ones.

A preliminary K_d measurement on samples calcined at different temperatures showed $K_d(HPO_4^{2-})$ values of 500, above 10^4, and 2100 cm^3/g for MgMn-2-473, MgMn-2-573, and MgMn-2-673, respectively. Since MgMn-2-573 showed the highest K_d value, the phosphate adsorptive properties were studied using samples prepared at 573 K. Samples MgMn-2-573 and MgMn-6-573 have remarkably high K_d values for HPO_4^{2-} alone ($K_d > 10^4$ cm^3/g, adsorption rate > 99%). These calcined samples have lower $K_d(SO_4^{2-})$ values than the uncalcined samples. This indicates that the phosphate ion-sieve nature is strengthened by the calcination at 573 K. The XRD analysis of MgMn-2-573 after the K_d measurement showed that the amorphous structure was maintained after the K_d measurement. Any peaks corresponding to metal phosphate salts were not observed. Due to the low solubility of MgMn-LDH in alkaline solutions, the removal of phosphate ions by the dissolution–recrystallization reaction may rarely progress in the present case.

There are numerous references in the literature verifying the anion selectivity of different LDHs. Parker et al.[16] have reported anion selectivity in the order $SO_4^{2-} > F^- > HPO_4^{2-} > Cl^- > B(OH)_4^- > NO_3^-$ for MgAl-LDH. You et al.[26] also reported a high selectivity of HPO_4^{2-} for MgAl-LDH. In our previous study on oxo-anion exchange with different kinds of LDHs, we observed that MgAl-LDH can expand easily in aqueous solution.[27] Therefore, it can easily intercalate anions with large hydrated radii like SO_4^{2-}. Compared to MgAl-LDH, the present sample shows a relatively low selectivity for SO_4^{2-}. Since its anion exchange reaction progresses topotactically, maintaining the bulk and surface structure, SO_4^{2-} may be sterically excluded from the ion exchange sites due to its large hydrated radius. The strong phosphate ion-sieve capacity of calcined MgMn-LDH is advantageous for the removal of phosphate from waste water or seawater, since these solutions usually contain large amounts of SO_4^{2-} ions.

The pH-Dependence. The pH dependence of the phosphate uptake by MgMn-2-573 is shown in Fig. 6. The phosphate uptake increased with pH in the region below 8, and was maximum (1.1 mmol-P/g) at a pH around 8. The maximum phosphate uptake was nearly equal to half of the exchange capacity (2.1 mmol/g) derived from the chemical composition data. The phosphate uptake decreased with pH in the region pH > 9. MgAl-LDH and MgFe-LDH have shown similar pH-dependence profiles with maximum uptakes (1.9 and 1.4 mmol-P/g) around pH 7.[28,29] The present sample has a smaller phosphate uptake but stronger phosphate ion-sieve properties than these two.

Mechanism of Phosphate Adsorption. Phosphate ions exist in different ionic states including monovalent $H_2PO_4^-$, divalent HPO_4^{2-}, and trivalent PO_4^{3-} ions depending on the pH of the solution,[30]

$$H_3PO_4 \overset{K_1}{\rightleftharpoons} H_2PO_4^- + H^+ \overset{K_2}{\rightleftharpoons} HPO_4^{2-} + 2H^+ \overset{K_3}{\rightleftharpoons} PO_4^{3-} + 3H^+ \quad (2)$$

where $pK_1 = 2.15$, $pK_2 = 7.2$, and $pK_3 = 12.37$. The primary

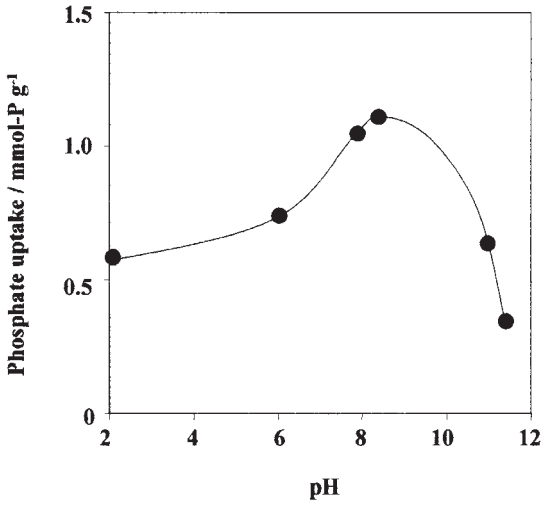

Fig. 6. Uptake of phosphate ions by MgMn-2-573 at different pH. Sample = 0.10 g, Concentration of NaH_2PO_4 = 4×10^{-3} M, Total vol. = 50 cm^3, Time = 3 d, Temp. = Room temp.

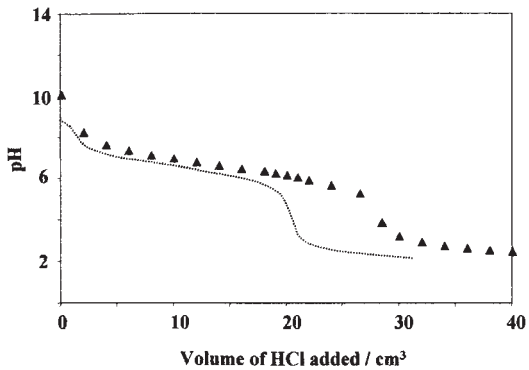

Fig. 7. pH titration curve of MgMn-2-573 with Na_2HPO_4. ▲: supernatant solution after the adsorption. Sample = 0.10 g, Conc. of Na_2HPO_4 = 0.1 M, Vol. of Na_2HPO_4 = 20 cm^3, Conc. of HCl = 0.1 M. Dotted line corresponds to blank titration.

ion is divalent HPO_4^{2-} at a pH around 8, thus we can expect a 2:1 HCO_3^-/HPO_4^{2-} exchange reaction since the main species of carbon is HCO_3^- in MgMn-2-573. To clarify the exchange reaction, the pH titration was carried out using a supernatant solution after phosphate adsorption (Fig. 7). The phosphate uptake by MgMn-2-573 was determined separately by analysis of the phosphate content of a solid sample as 0.92 mmol-P/g. The titration curve of the supernatant solution shows that the OH^-/HPO_4^{2-} exchange reaction rarely occurs during the HPO_4^{2-} adsorption, because the titration in the region pH > 8 (which corresponds to the titration of PO_4^{3-} produced by the reaction of OH^- with HPO_4^{2-}) is very small compared to those in the region at pH < 8. The inflection pH is around 4, which is nearly equal to that of blank titration. Since the dissociation constant ($pK_1 = 6.4$) of H_2CO_3 is close to that of $H_2PO_4^-$, nearly the same inflection pH between the two can be explained by the release of HCO_3^- from MgMn-2-573. The volume of HCl needed to reach the inflection point increases by 8 cm^3 from the blank titration, which corresponds to 0.8 mmol HCl

per gram of MgMn-2-573. This corresponds to more than 85% of the phosphate uptake. Therefore, we can conclude that HPO_4^{2-} adsorption for MgMn-2-573 progresses mainly by a 2:1 ion exchange of HCO_3^-/HPO_4^{2-}.

Conclusion

A systematic study of the preparative conditions of MgMn-LDHs was carried out. Pure and crystalline LDHs with a Mg/Mn ratio between 2 and 3 were obtained after oxidation of Mn(II) to Mn(III) species during the simultaneous precipitation of Mg(II) and Mn(II) in a mixed aqueous solution of NaOH and Na_2CO_3 in the temperature range between 275 and 313 K. The calcined MgMn-LDHs showed a specific selectivity towards phosphate ions alone, and are applicable as a new type of environmental adsorbent for aqueous phosphate ions in contaminated ecosystems.

References

1 S. Miyata, T. Kumura, H. Hattori, and K. Tanabe, *Nippon Kagaku Zasshi*, **92**, 514 (1971).

2 S. Miyata, *Clays Clay Miner.*, **28**, 50 (1980).

3 T. Sato, T. Wakabayashi, and M. Shimada, *Ind. Eng. Chem. Prod. Res. Dev.*, **25**, 89 (1986).

4 K. Okada, J. Temuujin, Y. Kameshima, and K. J. D. MacKenzie, *Mater. Res. Bull.*, **38**, 749 (2003).

5 S. Tanada, M. Kabeyama, N. Kawasaki, T. Sakiyama, T. Nakamura, M. Araki, and T. Tamura, *J. Colloid Interface Sci.*, **257**, 135 (2003).

6 J. M. Fernandez, C. Barriga, M.-A. Ulibarri, F. M. Labajos, and V. Rives, *J. Mater. Chem.*, **4**, 1117 (1994).

7 S. K. Yun and T. J. Pinnavaia, *Chem. Mater.*, **7**, 348 (1995).

8 S. Aisawa, S. Takahashi, W. Ogasawara, Y. Umetsu, and E. Narita, *J. Solid State Chem.*, **162**, 52 (2001).

9 S. Aisawa, H. Hirahara, H. Uchiyama, S. Takahashi, and E. Narita, *J. Solid State Chem.*, **167**, 152 (2002).

10 M. Adachi-Pagano, C. Forano, and J.-P. Besse, *Chem. Commun.*, **2000**, 91.

11 U. Costantino, N. Coletti, N. Nocchetti, G. G. Aloisi, F. Elisei, and L. Latterini, *Langmuir*, **16**, 10351 (2000).

12 A. Ookubo, K. Ooi, F. Tani, and H. Hayashi, *Langmuir*, **10**, 407 (1994).

13 A. Kawamoto, T. Suzuki, N. Kiba, and T. Sato, *J. Soc. Inorg. Mater., Jpn.*, **10**, 167 (2003).

14 R. W. Cargill, M. Dutkowsky, A. Prescott, L. W. Fleming, and W. K. Stewart, *J. Pharm. Pharmacol.*, **41**, 11 (1989).

15 B. E. Rittman, "Environmental Biotechnology," McGraw-Hill, Singapore (2001).

16 L. M. Parker, N. B. Milestone, and R. H. Newman, *Ind. Eng. Chem. Res.*, **34**, 1196 (1995).

17 P. J. Dunn, D. R. Peacot, and T. D. Palmer, *Am. Mineral.*, **64**, 127 (1979).

18 H. C. B. Hansen and R. M. Taylor, *Clay Miner.*, **26**, 507 (1991).

19 "Japan Industrial Standard (JIS)," M8233 (1982).

20 F. Cavani, F. Trifiro, and A. Vaccari, *Catal. Today*, **11**, 173 (1991).

21 J. P. Ramírez, G. Mul, and J. A. Moulijin, *Vib. Spectrosc.*, **27**, 75 (2001).

22 R. A. Nyquist and R. O. Kagel, "Infrared Spectra of Inorganic Compounds," Academic Press, New York and London (1971).

23 M. Abe, "Inorganic Ion Exchange Materials," ed by A. Clearfield, CRC Press, Boca Raton, Florida (1982), p. 161.

24 H. P. Boehm, *Angew. Chem.*, **78**, 617 (1966).

25 D. Reichenberg, "Ion Exchange," ed by J. A. Marinsky, Marcel Dekker, Inc., New York (1966), Vol. 1, p. 227.

26 Y. You, G. F. Vance, and H. Zhao, *Appl. Clay Sci.*, **20**, 13 (2001).

27 S. Tezuka, R. Chitrakar, A. Sonoda, K. Ooi, and T. Tomida, *Chem. Lett.*, **32**, 722 (2003).

28 A. Ookubo, K. Ooi, and H. Hayashi, *Langmuir*, **9**, 1418 (1993).

29 W. X. Zhang, H. Sakane, T. Hatsushika, N. Kinomura, and T. Suzuki, *J. Soc. Inorg. Mater., Jpn.*, (in Japanese), **4**, 132 (1997).

30 D. D. Perrin and B. Dempsey, "Buffers for pH and Metal Ion Control," Chapman and Hall, London (1974).